AIChE

On Packed Column Hydraulics

Brian Hanley
Research and Development, Aspen Technology, Inc., Burlington, MA 01803

DOI 10.1002/aic.12706
Published online July 21, 2011 in Wiley Online Library (wileyonlinelibrary.com).

Packed columns are normally operated countercurrently in the vapor-continuous regime. At specific combinations of liquid and vapor loads these columns flood. This article proposes that flooding is a form of second order (or "continuous") phase transition from vapor-continuous to liquid-continuous operation. Thus, flooding is unambiguously defined to be the set of those vapor/liquid flow combinations, $\{C_L, C_{Sf}\}$, that cause a liquid cluster to form that spans the diameter of column. These statements imply that a law of corresponding hydraulic states exists for packed columns. By this, we mean that sets of $\{C_L, C_S, (\Delta p/Z)_{2\phi}\}$ data taken with a specific packing and a specific vapor/liquid system exhibit a significant collapse when they are renormalized to $\{f_L, (\Delta p/\rho_L g Z)_{2\phi}\}$ (where f_L is the fractional approach to flood at constant liquid load). The renormalized dataset then applies to any vapor/liquid system using that particular packing. Renormalization thus forms the basis of a method for predicting column pressure drops and flood points for any column using the particular packing being studied. We demonstrate how the renormalization procedure is carried out by analyzing readily available air/water data for a number of different packings. We then show that a version of the Wallis equation can be used to correlate packed column flooding data successfully. Further, we demonstrate that the variation of the Wallis parameters with the equivalent diameters of packings in a geometrically similar family leads to a complete characterization of the effects of the physical properties of liquid on the flooding locus for these packings through the Bond number. This last result is a direct result of generalized homogeneity considerations. Finally, we show that there exists an even more general formulation of the law of corresponding hydraulic states that applies to all packings regardless of type, size, or material of construction.
 AIChE J, 58: 1671–1682, 2012
Keywords: packed column, pressure drop, flood, phase transition, renormalization

Introduction

Packed columns operated countercurrently in the vapor-continuous regime can reach points of hydraulic inoperability referred to as "flood points" or "maximum operating capacities" (occasionally, a degradation in the separation performance of the column precedes hydraulic inoperability; in that case, the upper limiting flows are referred to as maximum efficient capacities). Classical flooding is associated with a sharp rise in the pressure drop, a conspicuous loss in separation efficiency, an abrupt increase in the liquid holdup, and difficulty in maintaining stable column operation. These obvious symptoms conceal the difficulties engineers have had in proposing a complete and unambiguous mathematical definition for flood. For example, Kister and Gill[1] have found that there are over 20 operational definitions of flooding currently in use by the engineering community with no one of them satisfactory under all circumstances. This has led to a good deal of misunderstanding.

Even though a considerable body of experimental and theoretical work has been done to try to relate the set of vapor and liquid loadings at flood to parameters such as the geometrical characteristics of packing (hydraulic diameter, void fraction, and specific surface area) and the physical properties of liquid (shear or kinematic viscosity, density, and surface tension), a reliable picture for flooding in packed columns has not emerged. There is today no public domain model that is completely adequate for process design. Sanchez and Seibert[2] recently compared the predictions of several popular pressure drop correlations found in the open literature with available experimental data.[3–6] Their results are summarized in Figure 1 (A.F. Seibert, personal communication, 2003). It is clear that none of these correlations perform particularly well estimating packing pressure drops. The parity plots demonstrate that these correlations can be expected to achieve prediction accuracies of approximately ±40% on average over the range of variables investigated with a rather large variance about this mean. This level of accuracy is inadequate for industrial process design purposes. To be sure, the inclusion of system factors and foaming factors at the design level even today is largely a result of the failure of current models to accurately predict flooding envelopes for the wide variety of systems encountered in the chemical industry.[8]

Hanley et al.[9] proposed that flooding for most columns in the low to intermediate liquid load regime can be explained in terms of a second order phase transition from vapor-continuous to liquid-continuous operation (the mirror transition is also possible, because at high liquid loads, it is possible for columns to operate in a liquid-continuous mode).

Correspondence concerning this article should be addressed to B. Hanley at brian.hanley@aspentech.com.

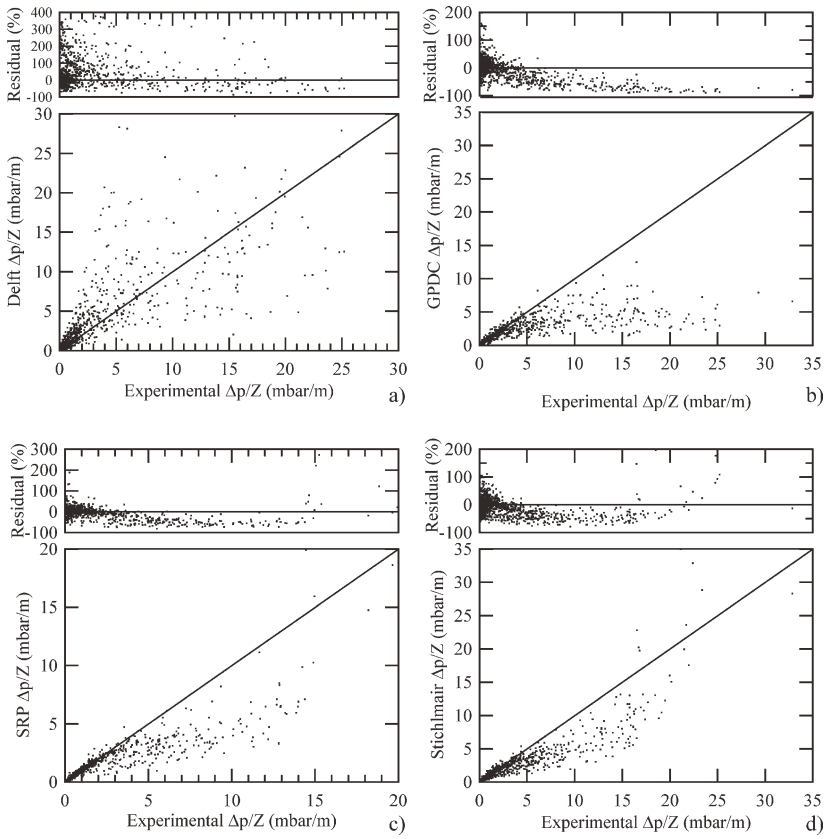

Figure 1. Parity plots of predicted pressure drop vs. reported experimental pressure drop for four pressure drop models found in the open literature (A.F. Seibert, personal communication, 2003).[2]

(a) the Delft model for structured packings,[3] (b) the generalized pressure drop correlation (GPDC),[7] (c) the SRP, or Bravo, Rocha, and Fair model for structured packings,[6] and (d) the model of Stichlmair et al.[4]

Additionally, these authors used the Wallis equation[10] as modified by McNulty and Hsieh,[11] $\sqrt{C_{Sf}} + m\sqrt{C_L} = c$, to correlate liquid and vapor loads at flood*. The authors recognized that the form of the Wallis equation given above was incomplete because it did not account for the effect of liquid physical properties on the flooding locus except in an *ad hoc* way. One goal of this article is to remedy that deficiency.

Data Analysis

It is the contention of this article that flooding in columns operated countercurrently at low to intermediate liquid loadings represents a second order phase transition from vapor-continuous to liquid-continuous operation. Phase transitions in physical systems have been an active area of scientific investigation for at least 200 years. The lay person is undoubtedly familiar with solid/liquid/vapor transitions such as those that occur between ice, water, and steam. However, phase transitions occur in many other types of systems– for example, the transition from ferromagnetic behavior to paramagnetic behavior for ferromagnets at the Curie temperature or the conductor/insulator, conductor/superconductor, or conductor/semiconductor percolation thresholds for electrical networks.[12–14]

Phase transitions are classified as being either first-order or continuous (or, more infrequently, second-order) transitions. First-order transitions involve the evolution or absorption of heat at the transition point. In contrast, continuous transitions are not accompanied by a heat effect. In addition, continuous phase transitions are accompanied by the growth of fluctuations on ever longer length scales[15] (recall that packed columns exhibit large performance fluctuations as flooding is approached). Transitions are further organized into groupings called universality classes. For systems from the same universality class, renormalizing raw experimental data taken near the critical point to the proper critical conditions has the remarkable effect of collapsing all of these data, regardless of the experiment, onto what is essentially a master curve.[12,16,17] For example, the critical exponents for the λ transition of a fluid/superfluid system are found to be an exact match for the critical exponents of the paramagnetic/ferromagnetic phase transition in uniaxial ferromagnets. The qualification that universality is observed only near critical points is often an unnecessary restriction. "Near" is very often found to mean the entire range of observable experimental data.

The flooding phenomenon in packed columns is extremely complex. It is possible to operate a column away from flooding in either vapor-continuous or liquid-continuous mode. The crossover from normal vapor-continuous operation to something more akin to operation in a liquid-continuous mode is signaled by the onset of a change in slope of the pressure drop vs. vapor velocity away from flooding. Consider Figure 2. Displayed is the typical behavior of the pressure drop as a function of the vapor's F_S at various fixed liquid loadings with $L_4 > L_3 > L_2 > L_1$. Included on the figure are lines with the same power law slope—$\partial[\ln(\Delta p/H)]/\partial[\ln(F_S)]|_L$—as that for the dry pressure drop placed over each of the two phase

*Estimate based on best available information.

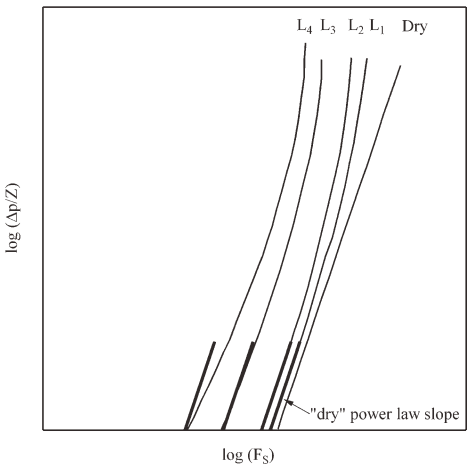

Figure 2. Illustration showing how to determine the maximum liquid loading appropriate for inclusion in the analysis methodology presented in this article.

pressure drop curves away from flooding. The initial power law slopes for the curves labeled L_1, L_2, and L_3, are nearly the same as that for the dry pressure drop. However, there is a noticeable difference in the two slopes for the curve with liquid load L_4. Clearly, by liquid load L_4, the behavior of the pressure drop away from macroscopic flooding has changed in some fashion. Therefore, the analysis of this article is limited to liquid loadings below L_4, where L_4 is typically on the order of 100 $m^3/m^2 \cdot h$ ($\sim$40 gpm/ft^2).

Earlier packed column researchers recognized the fundamental nature of the phase inversion and its connection to macroscopic flooding, but they did not make the connection to the statistical physics of critical phenomena in their analyses.[18–21] The vapor/liquid phase transition in a packed column is geometrical rather than thermal in nature. Locally, pockets of liquid build up in the voids of the column. As the operating conditions of the column are changed to bring it closer to macroscopic flooding more of the voids become filled with liquid. Clustering begins to occur among the liquid filled voids. Macroscopic flood occurs when the connectivity of the liquid clusters is such that one of the clusters spans the column diameter. Therefore, the mathematics describing phase inversion flooding in a packed column should be very similar in character to that for the description of phase transitions in percolating systems.

We begin by assuming that the pressure drop curves for individual liquid loadings as depicted in Figure 2 belong to the same universality class and that the pressure drop at flood is independent of the liquid load. These conjectures imply that individual curves of $(\Delta p/Z)_{2\phi}$ vs. F_S at constant liquid load should collapse onto a common curve when the vapor F_S values are properly renormalized to the vapor F_S at flood, F_{Sf}, for a given liquid load. The resultant abscissa value, F_S/F_{Sf}, is the fractional approach to flood at constant liquid load, hereafter referred to as f_L. We refer to this as the hypothesis of corresponding hydraulic states for packed columns. Note that $F_S/F_{Sf} = C_S/C_{Sf}$. Hereafter, we shall use C_S/C_{Sf} to represent f_L. This choice will be explained below. In addition to the above assumption, we use the fact that all correctly formulated equations describing physical phenomena must be dimensionally consistent. This last statement implies that there exists a form for the equation describing pressure drop and flooding in packed columns that is dimensionless. The new abscissa—the fractional approach to flood at constant liquid load—is already dimensionless. There are two potential choices for the appropriate renormalization factor for the ordinate, $(\Delta p/Z)_{2\phi}$, suggested by the problem's physics. These are the dry pressure drop per unit height at the same F_S, $(\Delta p/Z)_{dry}$, or the pressure drop per unit height due to the static head of liquid, $\rho_L g$. Because of the dependence of $(\Delta p/Z)_{dry}$ on F_S, the scaled dimensionless ordinate $[(\Delta p/Z)_{2\phi}/(\Delta p/Z)_{dry}]$ destroys the empirical data collapse already observed. On the other hand, the static head of liquid, $\rho_L g$, is a constant in these types of experiments and so the scaled dimensionless ordinate $[(\Delta p/Z)_{2\phi}/\rho_L g]$ preserves the desired data collapse. Therefore,

$$\left(\frac{\Delta p}{\rho_L g Z}\right)_{2\phi} = P\left(\frac{C_S}{C_{Sf}(C_L)}\right) = P(f_L) \tag{1}$$

Note that the statements above refer to column hydraulics alone. No mention has been made of the packing's separation efficiency, as with the maximum efficient (or useful) capacity or maximum operating capacity concepts and their attendant difficulties.[8,22–24]

A graphical depiction of the anticipated results of proper data reduction is shown in Figure 3 for the specific case of $(\Delta p/\rho_L g Z)_{2\phi}$ vs. C_S for four different liquid loads. With the proper choice of values for the four vapor loadings at flood—C_{Sf1}, C_{Sf2}, C_{Sf3}, and C_{Sf4}—a significant collapse of data should be apparent when the data are replotted with the new abscissas for each liquid load defined as approach to flood at constant liquid load—C_S/C_{Sf1}, C_S/C_{Sf2}, C_S/C_{Sf3}, and C_S/C_{Sf4}. This observation leads to the following strategy for

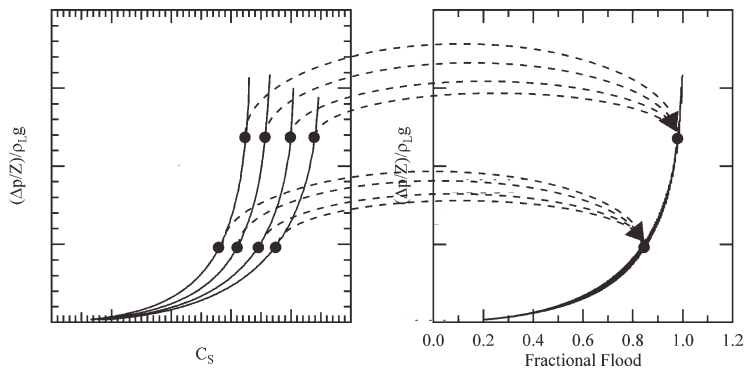

Figure 3. Pictorial depiction of the data renormalization procedure used in this article.

finding flooding velocities: flooding velocities are those which minimize the total variance (or total standard deviation) in the calculated fractions of flood among all sets of points with constant pressure drop. For a single set of four points, we would choose the flooding rates—C_{Sf1}, C_{Sf2}, C_{Sf3}, and C_{Sf4}—so that they minimize the expression for the standard deviation, σ:

$$\sigma\left((\Delta p/\rho_L g Z)_{2\phi}=V_1\right)=\sqrt{\frac{\left(f_{L(1,V_1)}-\left\langle f_{L(V_1)}\right\rangle\right)^2+\left(f_{L(2,V_1)}-\left\langle f_{L(V_1)}\right\rangle\right)^2+\left(f_{L(3,V_1)}-\left\langle f_{L(V_1)}\right\rangle\right)^2+\left(f_{L(4,V_1)}-\left\langle f_{L(V_1)}\right\rangle\right)^2}{3}}$$

where

$$f_{L(1,V_1)}=\frac{\left(C_{S1}|_{(\Delta p/\rho_L g Z)_{2\phi}=V_1}\right)}{C_{Sf1}}$$
$$f_{L(2,V_1)}=\frac{\left(C_{S2}|_{(\Delta p/\rho_L g Z)_{2\phi}=V_1}\right)}{C_{Sf2}}$$
$$f_{L(3,V_1)}=\frac{\left(C_{S3}|_{(\Delta p/\rho_L g Z)_{2\phi}=V_1}\right)}{C_{Sf3}} \quad (3)$$
$$f_{L(4,V_1)}=\frac{\left(C_{S4}|_{(\Delta p/\rho_L g Z)_{2\phi}=V_1}\right)}{C_{Sf4}}$$

and

$$\left\langle f_{L(V_1)}\right\rangle=\frac{f_{L(1,V_1)}+f_{L(2,V_1)}+f_{L(3,V_1)}+f_{L(4,V_1)}}{4} \quad (4)$$

$(\Delta p/\rho_L g Z)_{2\phi}=V_1$ is the value of the dimensionless pressure drop for which we wish to estimate flooding velocities; $C_{Si}|_{(\Delta p/\rho_L g Z)_{2\phi}=V1}$ represents the value of C_S for the liquid load numbered "i" (in this case, $1 \le i \le 4$) corresponding to a reduced pressure drop $(\Delta p/\rho_L g Z)_{2\phi}=V_1$, $f_{L(i,\,V_1)}$ is the value of the approach to flood for the liquid load numbered "i" at a dimensionless pressure drop of V_1, and $\langle f_{L(V_1)}\rangle$ is the average of the four $f_{L(i,\,V_1)}$ values.

In general, for "N_{C_L}" individual liquid loads (numbered 1 through N_{C_L}):

$$\sigma\left((\Delta p/\rho_L g Z)_{2\phi}=V_i\right)=\sqrt{\frac{1}{N_{C_L}-1}\sum_{j=1}^{N_{C_L}}\left(\frac{\left(C_{Sj}|_{(\Delta p/\rho_L g Z)_{2\phi}=V_i}\right)}{C_{Sfj}}-\left\langle f_{L(V_i)}\right\rangle\right)^2} \quad (5)$$

where

$$\left\langle f_{L(V_i)}\right\rangle=\frac{1}{N_{C_L}}\sum_{j=1}^{N_{C_L}} f_{L(j,V_i)} \quad (6)$$

To determine the set of C_{Sf} values that best renormalize the pressure drop data, we must minimize the sum of the standard deviations for all values of $(\Delta p/\rho_L g Z)_{2\phi}=V_i$ with respect to the set $\{C_{Sfj} : 1 \le j \le N_{C_L}\}$:

$$\sum_{V_i}\sigma\left((\Delta p/\rho_L g Z)_{2\phi}=V_i\right)=\sum_{V_i}\sqrt{\frac{1}{N_{C_L}-1}\sum_{j=1}^{N_{C_L}}\left(\frac{\left(C_{Sj}|_{(\Delta p/\rho_L g Z)_{2\phi}=V_i}\right)}{C_{Sfj}}-\left\langle f_{L(V_i)}\right\rangle\right)^2} \quad (7)$$

At least one flooding velocity needs to be fixed at the start of the fit, since any multiple of the actual flood velocities will also collapse the data. Least squares can be used to perform the optimization by setting the objective function to be zero for all points (we want the standard deviation or variance to be as close to zero as possible). The procedure as outlined above assumes that constant pressure drop data across several liquid loads are readily available. In terms of raw data, this will rarely be true—experiments are usually not performed in a mode wherein pressure drops are held constant, while vapor load is varied at constant liquid load. Instead, most experiments hold the liquid load constant while scanning across the vapor load. Pressure drop is the measured variable. The required constant pressure drop data can be estimated in a number of ways. For example, smooth curves can be drawn through the data and then points at constant pressure drop read off. Alternatively, one could incorporate some type of numerical interpolation procedure (linear interpolation, cubic spline interpolation, or smoothing spline interpolation, for example) into the least squares routine. In the data analyses performed below, we used linear interpolation on $\ln((\Delta p/\rho_L g Z)_{2\phi})$ vs. $\ln(C_S)$.

Results

We have carried out the procedure described above for air/water data on approximately 200 individual packings, including both random and structured types.[25–47] In the great majority of cases, the data collapse as described above quite well. Figure 4 contains examples demonstrating that the data collapse occurs for several different packing types across a range of different vendors.[26–28,30,39,43] However, cases do occur where the proposed collapse is less than satisfactory. Two examples are given in Figure 5 for IMTP #25 and for FLEXIPAC 1YHC.[30,31] It is unclear why certain datasets fail to collapse as expected. It is possible, given the difficulty of performing these types of experiments well, that the datasets themselves are simply in error, perhaps because of flow meter and/or pressure transducer miscalibrations or perhaps because of water in the tap lines leading to the pressure transducer diaphragms. Other causes might include liquid maldistribution caused by an out-of-level distributor or, in the case of structured packings, incorrect installation of the wall wipers.

Extension to other chemical systems

Dimensional Analysis The analysis above has demonstrated that the dimensionless pressure drop for a packed bed, $(\Delta p/\rho_L g Z)_{2\phi}$, is a function only of the approach to flood at constant liquid load, f_L for the great majority of air/water experiments examined (Eq. 1). The extension of these results to systems other than air/water is of paramount importance. Equation 1 can be rewritten more explicitly as follows:

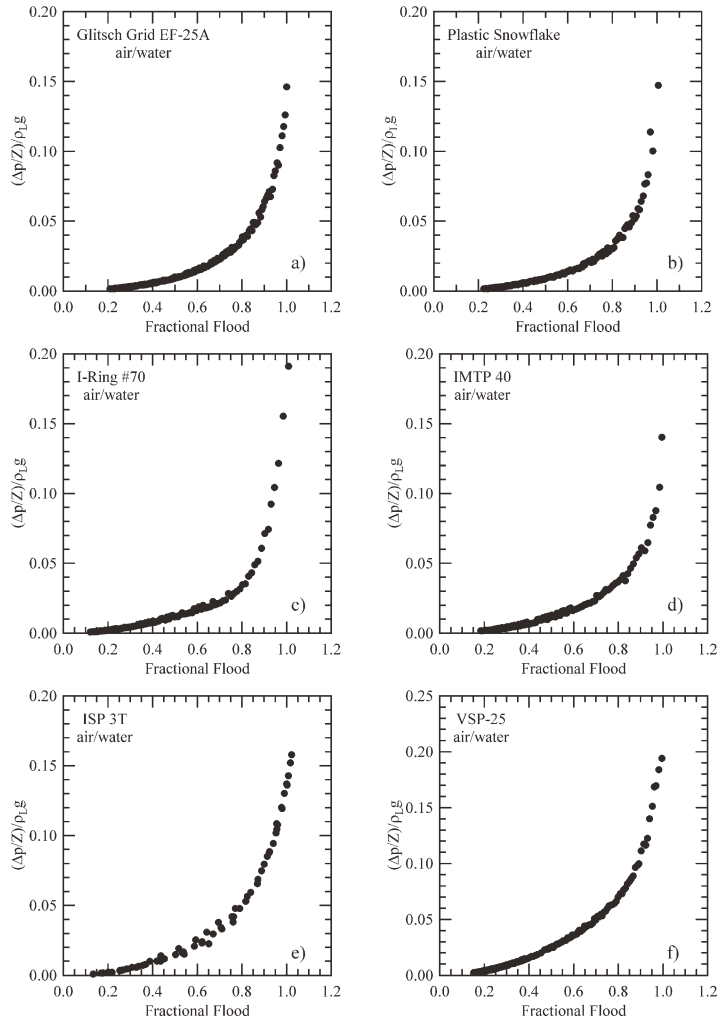

Figure 4. Renormalized air/water data for several packings.

(a) Glitsch Grid EF-25A[26] A metal structured packing,[27] (b) plastic Snowflake random packing,[25] (c) #70 I-Ring metal random packing,[28] (d) IMTP 40 metal random packing,[30] (e) ISP 3T metal structured packing,[43] and (f) metal VSP-25 random packing.[39]

$$\left(\frac{\Delta p}{\rho_L g Z}\right)_{2\phi} = P\left(\frac{C_S}{C_{Sf}(C_L, \mu_L, \sigma, \rho_L, g, d_e)}\right) \tag{8}$$

since it is well-known that the flooding vapor load at constant liquid loading for a given packing within a packing family depends on the liquid load, on the given packing's size, and on the physical properties of the liquid.[48–52] We see, through Eq. 8, that the two-phase pressure drop in one system can be calculated from two-phase pressure drop data taken with another system so long as vapor loadings at flood in the new system are available or can be deduced from flood data taken in the original system. Therefore, to apply air/water data to other systems, we must understand how the vapor load at flood, C_{Sf}, depends on packing size, liquid loading, and physical properties of the liquid.

At this point, we introduce the Wallis equation[10] as modified and extended by McNulty and Hsieh[11] for the description of flooding in packed columns. The Wallis equation is a semitheoretical flooding relation derived for vapor/liquid countercurrent flow in circular tubes; with modifications, McNulty and Hsieh found that Wallis equation can also be applied successfully to the correlation of packed column flood data.[11,53,54]

$$\sqrt{C_{Sf}} + m\sqrt{C_L} = c \tag{9}$$

The fact that the Wallis equation more directly relates C_{Sf} to C_L rather than F_{Sf} to C_L explains our earlier preference for using $f_L = C_S/C_{Sf}$ rather than the more intuitive $f_L = F_S/F_{Sf}$.

To account for the known effect of packing size and of the physical properties of liquid on flood within a given packing family, we assume that the Wallis parameters are functions of the physical properties of liquid and the size of packing:

$$c = c(\mu_L, \sigma, \rho_L, g, d_e) \tag{10}$$

$$m = m(\mu_L, \sigma, \rho_L, g, d_e) \tag{11}$$

where μ_L is the shear viscosity of the liquid, σ is the surface tension, ρ_L is the liquid's density, g is the acceleration of gravity, and d_e is the equivalent diameter of packing, defined here to be $d_e = 4\varepsilon/a$. Dimensional consistency requires that:[55,56]

$$c = (g d_e)^{\frac{1}{4}} C\left(\left(\frac{\rho_L^2 d_e^3 g}{\mu_L^2}\right), \left(\frac{\rho_L d_e^2 g}{\sigma}\right)\right) \tag{12}$$

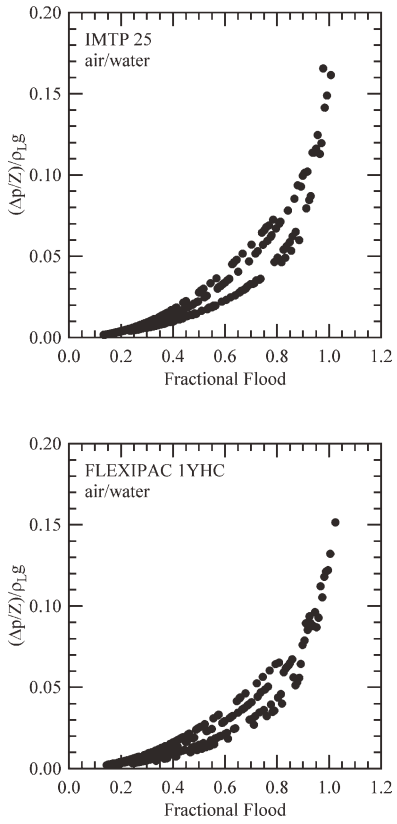

Figure 5. Renormalized air/water data for IMTP #25 random packing and FLEXIPAC 1YHC illustrating poor or incomplete data collapse.[30,31]

$$m = M\left(\left(\frac{\rho_L^2 d_e^3 g}{\mu_L^2}\right), \left(\frac{\rho_L d_e^2 g}{\sigma}\right)\right) \tag{13}$$

$$\mathrm{Ga} = \left(\frac{\rho_L^2 d_e^3 g}{\mu_L^2}\right) \tag{14}$$

$$\mathrm{Bo} = \left(\frac{\rho_L d_e^2 g}{\sigma}\right) \tag{15}$$

We shall further assume that the Wallis equation coefficients are simple power laws of the Galilei number and the Bond number:

$$c = c_0 (g d_e)^{\frac{1}{4}} \mathrm{Ga}^{\xi} \mathrm{Bo}^{\psi} \tag{16}$$

$$m = m_0 \mathrm{Ga}^{\kappa} \mathrm{Bo}^{\varpi} \tag{17}$$

The analysis above implies that:

$$C_{Sf} = \left(c_0 (g d_e)^{\frac{1}{4}} \mathrm{Ga}^{\xi} \mathrm{Bo}^{\psi} - m_0 \mathrm{Ga}^{\kappa} \mathrm{Bo}^{\varpi} \sqrt{C_L}\right)^2 \tag{18}$$

and that, therefore,

$$f_L = \left(\frac{C_S}{C_{Sf}(C_L, \mathrm{Ga}, \mathrm{Bo})}\right) = \frac{C_S}{\left(c_0 (g d_e)^{\frac{1}{4}} \mathrm{Ga}^{\xi} \mathrm{Bo}^{\psi} - m_0 \mathrm{Ga}^{\kappa} \mathrm{Bo}^{\varpi} \sqrt{C_L}\right)^2} \tag{19}$$

Note that only the Galilei number contains the kinematic viscosity of liquid and that only the Bond number contains the surface tension of liquid. This leads to some important conclusions. For example, if either or both of the dimensionless Wallis equation coefficients, $c/(gd_e)^{1/4}$ or m, depend on equivalent diameter in air/water experiments (by far the most commonly performed), then this immediately implies that they also must depend on some or all of the physical properties of liquid. Figure 6 illustrates the variation of "c" and "m" with equivalent diameter, d_e, in air/water experiments for metal FLEXIRINGS and metal FLEXIPAC structured packing in the "X" configuration.

Two potentially limiting cases arise: (a) flooding does not depend on the ratio of the liquid density to the surface tension, and (b) flooding does not depend on the kinematic viscosity. In the first case, the kinematic viscosity dependence of the Wallis coefficients can be obtained immediately from a set of air/water experiments with different sizes of packings in the same family (through the Galilei number). In the second, the liquid density and surface tension dependence of the Wallis coefficients can be obtained in the same way from a set of air/water experiments with different sizes of packings in the same family. The most general case—where the flood point depends on the kinematic viscosity, liquid density, and surface tension—would require that testing be done in more than the standard air/water system.

To investigate the dependence of the flood point on the Galilei number and/or the Bond number, we have collected some reported flood point data from standard total reflux distillation experiments for several packing styles and sizes and summarized them in Table 1.[24,57–59] In addition, reported flood points from several nonaqueous hydraulic experiments with air or natural gas can be found in Table 1.[60,61] These flood data are plotted in Figure 7 as percentage error in the predicted flood point vs. (a) the Galilei number or (b) the Bond number. Clearly a dependence of the Wallis coefficients on the Galilei number alone can result in unacceptably large errors in the predicted values of C_{Sf}; the average error in the predicted flood points is approximately 12% with a standard deviation close to 30. The situation is noticeably improved for the case of the Wallis coefficients being functions of Bond number; the average error in this case is −1.4% with a standard deviation of 8.8. It seems fair to conclude, then, that the Wallis coefficients are functions of the Bond number alone. This observation implies that the vapor rate at flooding, C_{Sf}, is a function of the liquid density and the surface tension. On the other hand, the generalized pressure drop correlation (GPDC) predicts that C_{Sf} is a function of the liquid density and the liquid viscosity.[5,7,18,49]

The final expression for the two phase pressure drop for a packed column in terms of its geometry and in terms of the physical properties of the liquid phase is given by Eq. 20.

$$\left(\frac{\Delta p}{\rho_L g Z}\right)_{2\phi} = P(f_L)$$
$$f_L = \frac{C_S}{\left(c_0 (g d_e)^{\frac{1}{4}} \mathrm{Bo}^{\psi} - m_0 \mathrm{Bo}^{\varpi} \sqrt{C_L}\right)^2} \tag{20}$$

Table 2 lists values of the Wallis equation correlating parameters c_0, ψ, m_0, and φ found in Eq. 20 for several different packing families.

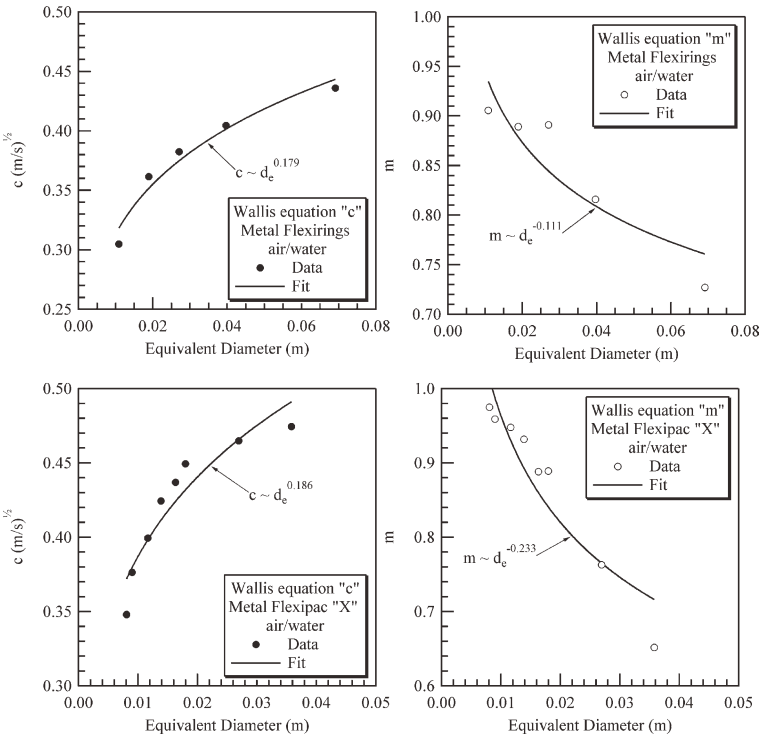

Figure 6. Top row: Variation of the Wallis parameters with equivalent diameter for metal FLEXIRINGS[41]; bottom row: variation of the Wallis parameters with equivalent diameter for metal FLEXIPAC "X" style structured packings.[43]

Table 1. Comparison of Experimental Flooding Velocities with Values Calculated from Air/Water Data using Either the Galilei Number or Bond Number to Correct for Physical Property Effects (see Eq. 19)

			C_{Sf}	C_{Sf}	C_{Sf}					% Error	% Error	
Packing	System	Pressure (kPa)	Experiment (m/sec)	Ga (m/sec)	Bo (m/sec)	ρ_L (kg/m^3)	ρ_V (kg/m^3)	μ_L (kg/m·sec)	σ (N/m)	Ga	Bo	References
ISP 1T	i-C8/tol.	98.7	0.085	0.086	0.087	645.010	3.499	2.357E-04	0.013	0.906	2.607	23
ISP 1T	i-C8/tol.	13.3	0.107	0.109	0.105	686.784	0.568	3.941E-04	0.018	1.556	−1.714	23
ISP 1T	EB/Sty	6.7	0.114	0.114	0.114	840.586	0.257	4.416E-04	0.026	−0.101	0.331	23
ISP 2T	i-C8/tol.	98.7	0.112	0.101	0.102	645.010	3.499	2.357E-04	0.013	−10.102	−8.596	23
ISP 2T	i-C8/tol.	13.3	0.131	0.128	0.124	686.784	0.568	3.941E-04	0.018	−2.216	−5.349	23
ISP 2T	C6/C7	33.3	0.134	0.122	0.123	833.051	0.989	4.301E-04	0.025	−8.679	−8.336	23
ISP 2T	C6/C7	107	0.116	0.105	0.109	787.336	2.895	2.936E-04	0.020	−9.485	−5.796	23
ISP 2T	C6/C7	165	0.110	0.099	0.104	766.602	4.299	2.541E-04	0.018	−10.225	−5.652	23
ISP 2T	C6/C7	413	0.110	0.086	0.091	713.265	9.862	1.863E-04	0.014	−21.859	−17.006	23
ISP 2T	EB/Sty	6.7	0.152	0.135	0.135	840.586	0.257	4.416E-04	0.026	−11.499	−11.118	23
ISP 3T	i-C8/tol.	98.7	0.119	0.111	0.113	645.010	3.499	2.357E-04	0.013	−6.637	−5.033	23
ISP 3T	i-C8/tol.	13.3	0.140	0.139	0.134	686.784	0.568	3.941E-04	0.018	−0.772	−4.018	23
ISP 4T	i-C8/tol.	98.7	0.122	0.110	0.111	645.010	3.499	2.357E-04	0.013	−10.189	−8.620	23
ISP 4T	i-C8/tol.	13.3	0.149	0.135	0.131	686.784	0.568	3.941E-04	0.018	−9.087	−12.101	23
MELLAPAK 250Y	CB/EB	101.325	0.086	0.099	0.102	769.006	3.174	2.348E-04	0.017	15.654	18.047	57
MELLAPAK 250Y	CB/EB	10.1325	0.121	0.122	0.123	837.663	0.382	4.034E-04	0.024	0.870	1.408	57
MELLAPAK 250Y	CB/EB	5.066	0.140	0.128	0.128	852.734	0.200	4.723E-04	0.026	−8.345	−8.597	57
IMTP 40	i-C8/tol.	101.325	0.095	0.091	0.092	645.010	3.499	2.357E-04	0.013	−4.777	−3.758	58
IMTP 40	EB/Sty	6.67	0.136	0.113	0.113	840.586	0.257	4.416E-04	0.026	−16.943	−16.721	58
CMR #1	Xylenes	6.67	0.100	0.108	0.109	828.240	0.256	4.162E-04	0.024	8.468	8.857	58
FLEXIPAC 250Y	TEG/C_4/H_2O	4582.90	0.147	0.210	0.147	1129.000	43.100	3.593E-02	0.045	42.911	0.147	60
25 mm Pall ring	Air/glycol	101.325	0.064	0.091	0.066	1113.000	1.135	1.800E-02	0.047	42.046	3.933	61
25 mm Pall ring	Air/glycol	101.325	0.059	0.085	0.062	1113.000	1.135	1.880E-02	0.047	43.649	4.757	61
25 mm Pall ring	Air/glycol	101.325	0.056	0.080	0.059	1113.000	1.135	1.860E-02	0.047	44.369	5.266	61
25 mm Pall ring	Air/oil	101.325	0.067	0.106	0.071	850.000	1.135	5.110E-02	0.026	58.816	5.596	61
25 mm Pall ring	Air/oil	101.325	0.059	0.097	0.065	850.000	1.135	5.230E-02	0.026	63.593	9.353	61
25 mm Pall ring	Air/oil	101.325	0.067	0.117	0.074	850.000	1.135	8.550E-02	0.023	73.485	10.541	61
25 mm Pall ring	Air/oil	101.325	0.061	0.108	0.069	850.000	1.135	8.920E-02	0.023	75.228	12.347	61

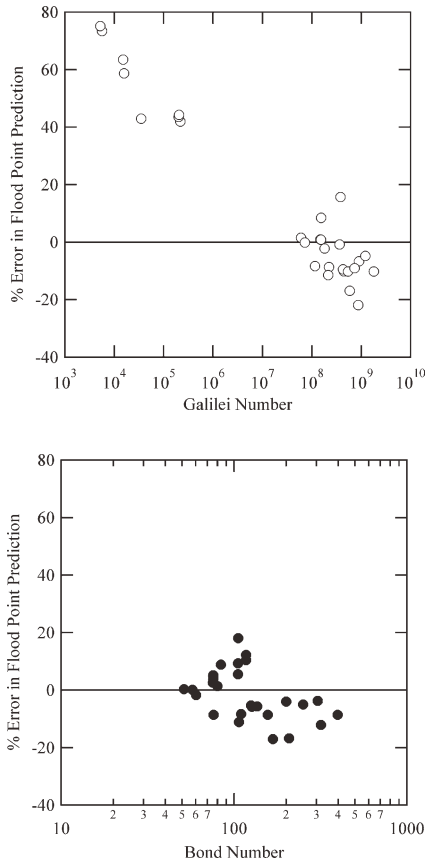

Figure 7. Data of Table 1 displayed as (a) percentage error in the calculated flood point vs. Galilei number; (b) percentage error in the calculated flood point vs. Bond number.

Data correlation

The functional form chosen to approximate $\mathbf{P}(f_L)$ for the purpose of data correlation should be flexible enough to fit data gathered from any packing style without difficulty using a relatively small number of correlating parameters. One such expression is:

$$P(f_L) = \alpha f_L^{(2-\beta\sqrt{f_L})}(\gamma - f_L)^{-\delta} \tag{21}$$

The rationale for the form of Eq. 21 is straightforward: far from flood, $\mathbf{P}(f_L)$ behaves like a power law with a power law exponent that is weakly dependent on the approach to flood. The exponent, $(2-\beta\sqrt{f_L})$, has a maximum value of 2, in line with the value for fully developed turbulent single phase flow. As flood is approached, the term $(\gamma - f_L)^{-\delta}$ comes into play and causes the pressure drop to turn upward, ultimately diverging at $f_L = \gamma$. The value of the coefficient γ, then, is always greater than one. Table 3 lists fitting coefficients for a number of different packings. Of course, other correlating expressions are possible.

Comparison to experiment

In Figure 8, we compare some experimental pressure drop data for nonaqueous distillation systems with predictions based on the analysis of air/water pressure drop data via the method described in this article.[24,62] In each case, the agreement is excellent up to and including flood. All calculations were performed using Aspen Technology's "*Aspen Rate-Based Distillation*" module with the countercurrent flow mode option.[63] In addition, the mass transfer correlations reported by Hanley and Shethna[64] and Hanley and Chen[65] were used in all calculations. All simulations were performed using the NRTL property package except those involving *i*-butane/*n*-butane where properties were calculated using Refprop.[66,67]

Data renormalization revisited

We have postulated that packed column flooding is a type of continuous phase transition and that the flooding mechanism for a particular packing is the same for every liquid load. Here, we examine the possibility that the flooding mechanism is not only the same for different liquid loads on the same packing but also the same, at some level, across every packing. This leads to the expectation that some higher level of symmetry exists in the data and that a more general type of data renormalization exists. For example, it is not difficult to find air/water datasets from packings with vastly different geometrical, topological, material, and flooding characteristics that superimpose once the raw data have been renormalized via the method of this article.

We begin by examining pressure drop/flooding data from two families of geometrically similar packings: FLEXIPAC in the "X" configuration (with a nominal channel inclination angle from the vertical of 30°) and FLEXIPAC in the "Y" configuration (with a nominal channel inclination angle from the vertical of 45°).[43] In Figure 9a, pressure drop data vs. fractional approach to flood for FLEXIPAC 1X, 1.4X, 1.6X, 2X, and 3X have been superimposed. Figure 9b is a similar plot for FLEXIPAC 1Y, 1.4Y, 2Y, 2.5Y, and 3Y. Similar data superpositions are shown in Figure 10a for the geometrically similar family of ISP structured packings—1T, 3T, 4T, and 5T—and in Figure 10b for the geometrically similar family Raschig Super Ring random packing family—#1, #2, and #3. These plots are a kind of new generalized pressure drop correlation for these four packing families. They reveal that the dimensionless pressure drop, $(\Delta p/\rho_L g Z)_{2\phi}$, is the same for all packings within a family at the same fractional approach to flood regardless of chemical system.

Perhaps even more surprising, data for packings dissimilar in size, geometry, and even material of construction, sometimes superpose on one another. Figure 11a contains data for ISP 3T metal structured packing, IMTP #60 random packing, FLEXERAMIC 88 ceramic structured packing, CMR 3A plastic random packing, metal Hy-Pak #3 random packing, 3″ ceramic Intalox saddles random packing, and metal Raschig Super Ring #2 random packing. Figure 11b is a plot in the same vein containing superimposed data for 25 mm Bialecki rings random packing, 2″ plastic Super Intalox saddles, 35 mm ceramic Raschig rings, metal VSP-25 random packing,

Table 2. Wallis Equation Coefficients for Various Packing Families (see Eq. 20)

Packing	c_0	$-\psi$	m_0	$-\omega$
Metal Nutter Rings	0.9219	0.0911	2.453	0.173
Metal IMTP	0.9442	.0969	2.667	0.198
Ceramic Intalox Saddles	0.5260	0.0127	1.253	0.114
Metal FLEXIPAC "Y"	0.6496	0.00349	1.575	0.110
Metal FLEXIPAC "X"	0.7518	0.0318	1.305	0.116
Metal FLEXIRING	0.6153	0.0356	1.0906	0.0556

Table 3. Equation 21 Correlation Parameters for Selected Packings

Packing	$\alpha \pm 1\sigma$	$\beta \pm 1\sigma$	$\gamma \pm 1\sigma$	$-\delta \pm 1\sigma$
1″ Metal FLEXIRING	0.02839 ± 0.0068	1.8782 ± 0.58	1.3152 ± 0.0916	1.4256 ± 0.562
2″ Metal FLEXIRING	0.04418 ± 0.0015	0.4142 ± 0.0548	1.053 ± 0.00312	0.4013 ± 0.0193
$3^1/_2$″ Metal FLEXIRING	0.04579 ± 0.000678	0.3558 ± 0.0242	1.0318 ± 0.00116	0.3501 ± 0.00754
Plastic Snowflake	0.008372 ± 0.000928	1.7803 ± 0.176	1.0773 ± 0.00577	1.1014 ± 0.074
FLEXERAMIC Type 88	0.02072 ± 0.000497	1.3328 ± 0.0375	1.0502 ± 0.00146	0.7056 ± 0.0142
FLEXERAMIC Type 28	0.01107 ± 0.000793	2 ± 0.114	1.0725 ± 0.0039	1.0327 ± 0.0473
IMTP #50	0.01657 ± 0.00128	1.4206 ± 0.121	1.0621 ± 0.00465	0.8304 ± 0.0486
IMTP #60	0.03778 ± 0.00098	0.3792 ± 0.0439	1.0346 ± 0.00158	0.3877 ± 0.0127
IMTP #70	0.01563 ± 0.000978	1.1876 ± 0.106	1.0381 ± 0.00233	0.6439 ± 0.0308
1″ Ceramic Raschig ring	0.1509 ± 0.0366	0	1.0318 ± 0.0168	0.3071 ± 0.114
β-ETA #1	0.05460± 0.00747	0.9278 ± 0.482	1.3848 ± 0.132	1.1186 ± 0.54
β-ETA #2	0.06354 ± 0.00329	0.1098 ± 0.0806	1.0839 ± 0.00994	0.3513 ± 0.0369
FLEXIPAC 1X	0.003604 ± 0.000327	2 ± 0.175	1.0325 ± 0.00127	1.0041 ± 0.038
FLEXIPAC 2X	0.004734 ± 0.000317	2 ± 0.123	1.0344 ± 0.00115	0.90603 ± 0.0292
FLEXIPAC 3X	0.005891 ± 0.0015	1.3239 ± 0.502	1.0385 ± 0.00512	1.0185 ± 0.118
FLEXIPAC 1Y	0.008666 ± 0.000712	2 ± 0.137	1.0353 ± 0.0025	0.8825 ± 0.0415
FLEXIPAC 2Y	0.008416 ± 0.000876	2 ± 0.17	1.0533 ± 0.0038	0.9653 ± 0.058
FLEXIPAC 3Y	0.01395 ± 0.00197	1.4662 ± 0.245	1.0437 ± 0.00489	0.7898 ± 0.072
25 mm Metal Bialecki ring	0.03590 ± 0.0111	1.6628 ± 0.527	1.0503 ± 0.0168	0.6037 ± 0.168
Metal VSP 25	0.02217 ± 0.00238	2 ± 0.168	1.1167 ± 0.0111	1.0527 ± 0.0945
Metal VSP 40	0.02873 ± 0.000976	1.2535 ± 0.051	1.0344 ± 0.00279	0.5745 ± 0.0205
Glitsch Grid EF-25A	0.02849 ± 0.000937	0	1.036 ± 0.0017	0.4798 ± 0.0162
FLEXIGRID 2	0.003064 ± 0.000505	2 ± 0.294	1.0973 ± 0.00495	1.3803 ± 0.101
FLEXIGRID 3	0.03046± 0.000768	0	1.0286 ± 0.00132	0.4654 ± 0.0123
2″ Plastic FLEXIRING	0.06651 ± 0.00148	0.2760 ± 0.0345	1.0562 ± 0.00348	0.3073 ± 0.0138

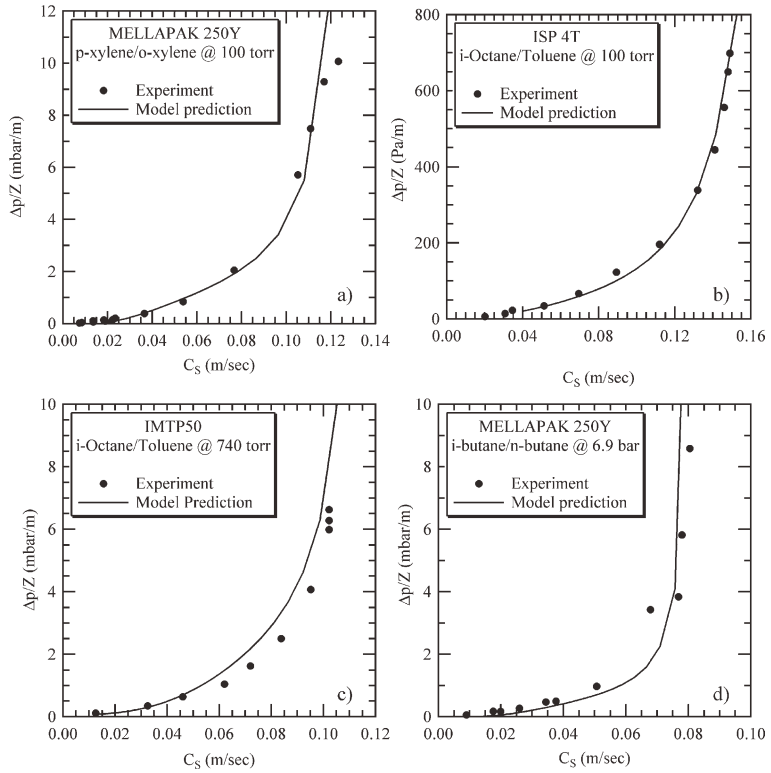

Figure 8. Comparison of experimental data with correlation predictions via the method outlined in this article.

(a) data of Fitz et al.[62] for the pressure drop of metal MELLAPAK 250Y structured packing vs. C_S for the xylenes system at 100 torr, (b) data of Rukovena and Koshy[24] for the pressure drop of metal ISP 4T structured packing vs. C_S for the system *i*-octane/toluene at 100 torr, (c) data of Rukovena and Koshy[24] for the pressure drop of IMTP #50 random packing vs. C_S for the system *i*-octane/toluene at 740 torr, and (d) data of Fitz et al.[62] for the pressure drop of metal MELLAPAK 250Y structured packing vs. C_S for the system *i*-butane/*n*-butane at 6.9 bar.

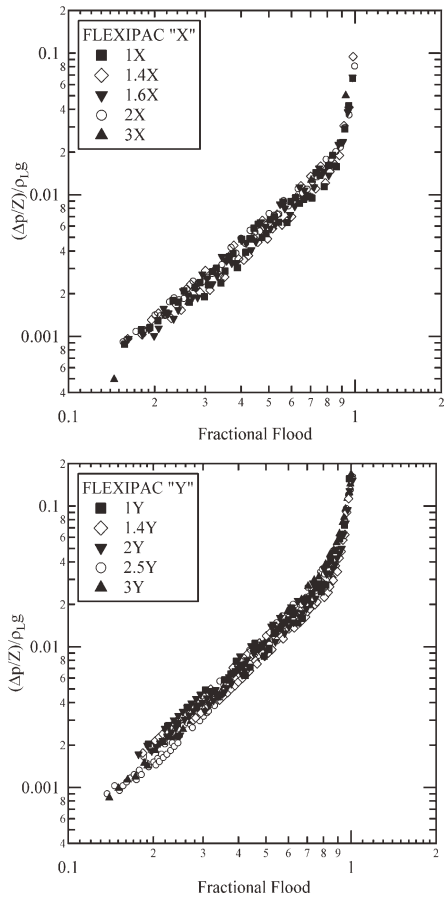

Figure 9. Examples of data superposition for packings within a family.

(a) Overlay plot showing data superposition for selected packing sizes from the FLEXIPAC "X" family of structured packings, and (b) overlay plot showing data superposition for selected packing sizes from the FLEXIPAC "Y" family of structured packings.[43]

metal Montz B1-500MN structured packing, 1″ ceramic Super Intalox saddles random packing, and 1″ metal Ballast rings random packing. Figure 12 is also similar and contains a superposition of pressure drop/flood data for different packings: metal FLEXIGRID 3 structured packing, metal FLEXIGRID 4 structured packing, Glitsch Grid EF-25A, plastic Snowflake random packing, metal FLEXIPAC 3Y structured packing, metal FLEXIPAC 4Y structured packing, and metal Twin-Pak #2 random packing. When Figures 11b and 12 are overlaid, as in Figure 13, for example, it becomes clear that these curves are distinct (as is the curve represented by the data superposition in Figure 11a, which was left out of the Figure 13 for clarity). It is currently unclear what distinctions among the various packings assign them to one curve or another. Visually, it appears as if the two curves diverge at different rates as they approach flood ($f_L = 1$). Critical point exponents for other types of geometrical phase transitions, like those found in bond or site percolation, can oftentimes be related to the network structure and the dimensionality of the space in which they occur. The different rates of divergence exhibited in Figures 11a, 11b, and 12 might be suggestive of differences in connectivity or some other topological parameter among the various packings. This finding requires further study.

Conclusions

The implications of the above analysis are potentially broad. The data analysis method described here most immediately leads to improved pressure drop and flood predictions for column design and rating. However, more importantly, it establishes that an underlying law of hydraulic corresponding states is a universal feature for pressure drop/vapor loading curves at constant liquid loading for an individual packing type. A further generalization of this underlying law of hydraulic corresponding states seems to operate for all of the packings belonging to the same packing family. In this case, the dimensionless two-phase pressure drop, $(\Delta p/\rho_L g Z)_{2\phi}$, becomes a function only of the fractional approach to flood, f_L. This finding leads to a kind of generalized pressure drop correlation for packing families that (a) dispenses with the need for packing factors for each packing size within a family and (b) properly deals with the effects of physical properties on the two-phase pressure drop and on the flood point for the packing. The Bond number scaling for the Wallis equation coefficients—based on rigorous dimensional analysis considerations—corrects to a very great degree the empirical physical property corrections of the various GPDC methods now in use. The most encouraging finding of this work is the suggestion that an even more encompassing form of hydraulic scaling exists that would include the

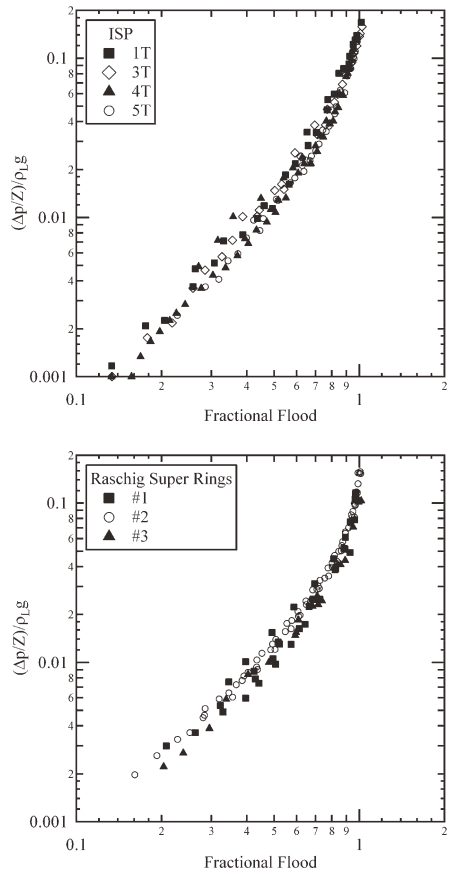

Figure 10. Examples of data superposition for packings within a family.

(a) Overlay plot showing data superposition for selected packing sizes from the metal ISP family of structured packings,[43] and (b) overlay plot showing data superposition for selected packing sizes from the Raschig Super Ring family of random packings.[41]

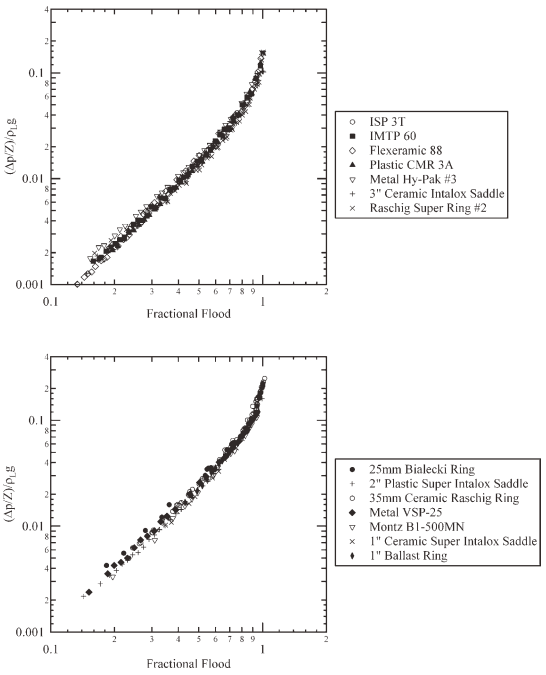

Figure 11. Examples of data superposition for dissimilar packings.

(a) Overlay plot showing data superposition for a number of unrelated packing sizes and styles; packings are listed in the caption,[26,29,30,41–43,69] and (b) overlay plot showing data superposition for a number of unrelated packing sizes and styles; packings are listed in the caption.[4,29,33,39,67]

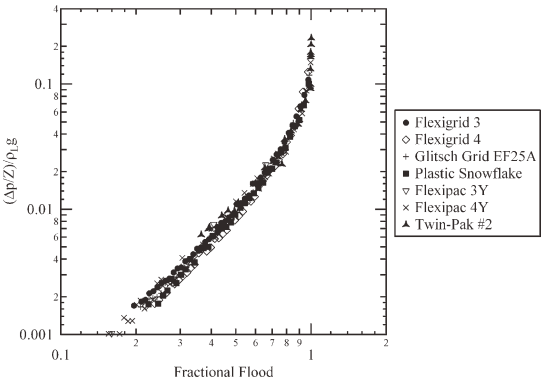

Figure 12. Overlay plot showing data superposition for several different packing types, sizes, and styles; packings are listed in the caption.[26,27,39,43]

hydraulic behavior of all packings regardless of size, configuration, or construction material.

Notation

a_d = dry specific packing area, m^2/m^3
Bo = Bond number
c = Wallis equation fitting parameter, $(m/sec)^{1/2}$
C_L = liquid superficial velocity, m/sec
C_S = density corrected superficial vapor velocity = $v_V\sqrt{\rho_V/(\rho_L-\rho_V)}$, m/sec
C_{Sf} = density corrected superficial vapor velocity at flood for a fixed liquid load, m/sec
D = column diameter, m

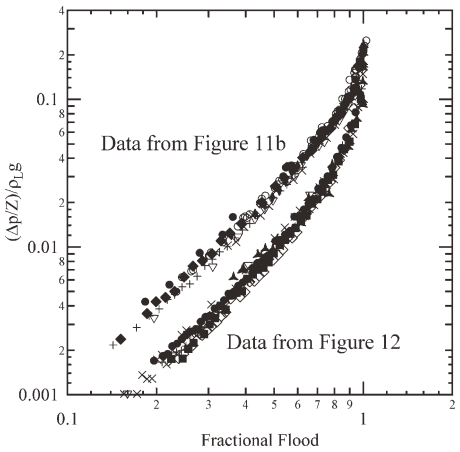

Figure 13. Comparison of Figures 11b and 12 illustrating the fact that the proposed law of corresponding hydraulic states for packings is incomplete.

d_e = equivalent diameter = $4\varepsilon/a_d$, m
f_L = fractional approach to flood at constant liquid loading
F_S = $v_V\sqrt{\rho_V}$, $Pa^{1/2}$
F_{Sf} = F_S value at flood for a fixed liquid load, $Pa^{1/2}$
g = acceleration of gravity, m/sec^2
Ga = Galilei number
L = superficial liquid flux, $kg/m^2{\cdot}sec$
m = Wallis equation fitting parameter
Z = packed bed depth

Greek letters

α = binary relative volatility
$(\Delta p/Z)_{2\phi}$ = two phase pressure drop per unit packed height, Pa/m
$(\Delta p/\rho_L gZ)_{2\phi}$ = dimensionless two phase pressure drop per unit packed height
ε = void fraction
μ_L = liquid viscosity, kg/m·sec
μ_V = vapor viscosity, kg/m·sec
ρ_L = liquid density, kg/m^3
ρ_V = vapor density, kg/m^3
σ = surface tension, N/m

Literature Cited

1. Kister HZ, Gill DR. Flooding and pressure drop prediction for modern random packings. Paper presented at AIChE Spring Meeting, 1990; Orlando, FL. March 18–22.
2. Sanchez P, Seibert AF. Pressure drop in packed distillation columns: evaluation of predictive models. Paper presented at: AIChE National Meeting, 2001; Reno, NV. November 4–9.
3. Olujić Ž. Development of a complete simulation model for predicting the hydraulic and separation performance of distillation columns equipped with structured packings. *Chem Biochem Eng Q*. 1997;11:31.
4. Stichlmair J, Bravo JL, Fair JR. General model for prediction of pressure drop and capacity of countercurrent gas/liquid packed columns. *Gas Separ Purif*. 1989;3:19–28.
5. Eckert JS. Selecting the proper distillation column packing. *Chem Eng Prog*. 1970;66:39–44.
6. Bravo JL, Rocha JA, Fair JR. Pressure drop in structured packings. *Hydrocarb Process*. 1986;56:45.
7. Ludwig EE. *Applied Process Design for the Chemical and Petrochemical Industries*. Vol 2. 3rd ed. Woburn: Butterworth-Heinemann, 1997.
8. Kister HZ. *Distillation Design*. New York: McGraw-Hill, 1992.
9. Hanley B, Dunbobbin B, Bennett D. A unified model for countercurrent vapor/liquid packed columns. 1. Pressure drop. *Ind Eng Chem Res*. 1994;33:1208–1221.
10. Wallis GB. *One-Dimensional Two-Phase Flow*. New York: McGraw-Hill, 1971.

11. McNulty K, Hsieh CL. Hydraulic performance and efficiency of Koch FLEXIPAC structured packings. Paper presented at: AIChE Annual Meeting, 1982; Los Angeles, CA. November 14–18.
12. Broadbent SR, Hammersley JM. Percolation processes I. Crystals and mazes. *Proc Camb Phil Soc*. 1957;53:629–641.
13. Hong DC, Stanley HE, Coniglio A, Bunde A. Random-walk approach to the two-component random-conductor mixture: perturbing away from the perfect random resistor network and random superconducting-network limits. *Phys Rev B*. 1986;33: 4564–4573.
14. Essam JW. *Percolation and cluster size*. In: Domb C, Greene MS, eds. *Phase Transitions and Critical Phenomena*. Vol 2. New York: Academic Press, 1972:197–270.
15. Binney JJ, Dowrick NJ, Fisher AJ, Newman MEJ. *The Theory of Critical Phenomena: An Introduction to the Renormalization Group*. Oxford: Oxford University Press, 1992.
16. Yeomans JM. *Statistical Mechanics of Phase Transitions*. Oxford: Clarendon Press, 1992.
17. Perry RH, Sliepcevich CM, Green DW, Kobayashi R, Leland TW. *Reaction kinetics, reactor design, and thermodynamics*. In: Perry RH, Chilton CH, Kirkpatrick SD, eds. *Perry's Chemical Engineers' Handbook*, 4th ed. New York: McGraw-Hill, 1963:4–49–4–55.
18. Eckert JS. A new look at distillation—4 tower packings comparative performance. *Chem Eng Prog*. 1963;59:76.
19. Lerner BJ, Grove CS. Critical conditions of two-phase flow in packed columns. *Ind Eng Chem*. 1951;43:216.
20. Zenz FA. What every engineer should know about packed tower operations. *Chem Eng*. 1953:176–184.
21. Krehenwinkel H, Knapp H. Pressure drop and flooding in packed columns operating at high pressures. *Chem Eng Technol*. 1987;10:231–242.
22. Dolan MJ, Strigle RF. Advances in distillation column design. *Chem Eng Prog*.78–83. November 1980.
23. Strigle RF, Rukovena F. Design of packed distillation columns. *Chem Eng Prog*. 1979:86–91. March 1979.
24. Rukovena F, Koshy TD. Packed distillation tower hydraulic design method and mechanical considerations. *Ind Eng Chem Res*. 1993;32:2400–2407.
25. Koch-Glitsch LP. Intalox Packed Tower Systems: Koch-Glitsch Random Packing. Vol KRP-5 3M0600B. Wichita, 2000.
26. Koch-Glitsch LP. Intalox Packed Tower Systems: Plastic Random Packing. Vol KGPP-1 2M050EE. Wichita, 2003.
27. Koch-Glitsch LP. Intalox Packed Tower Systems: Severe Services. Vol KGSS-1 2M0503E. Wichita, 2003.
28. Sulzer Chemtech. Metal Random Packing. Vol 22.64.06.40–VI.06–50. Winterthur.
29. Norton Chemical Process Products. *Design Information for Packed Towers*, 11th ed. Akron: Norton Chemical Process Products, 1971.
30. Koch-Glitsch LP. Intalox Packed Tower Systems: IMTP High Performance Packing. Vol KGIMTP-2 2M1303E. Wichita, 2003.
31. Koch-Glitsch LP. FLEXIPAC HC. Vol FPHC-3M0600B. Wichita, 2000.
32. Jaeger Products, Inc. Plastic Jaeger Rings and Saddles. Vol 700–0400-10000. Houston.
33. Julius Montz GmbH. High Performance Structured Packing. Vol GPS 10603503.
34. Verantis Environmental Solutions Group. Pressure Drop Vs. Gas Rate #2 Type-K Tellerette. Available at *www.verantis.com*; http://www.verantis.com/literature/12–10.13.pdf, accessed June 8, 2010.
35. Verantis Environmental Solutions Group. Pressure Drop Vs. Gas Rate #3 Type-R Tellerette. Available at *www.verantis.com*; http://www.verantis.com/literature/12–10.12.pdf, accessed 2009.
36. Verantis Environmental Solutions Group. Pressure Drop Vs. Gas Rate #3 Type K Tellerette. Available at www.verantis.com, accessed 2009.
37. Verantis Environmental Solutions Group. Pressure Drop vs. Gas Rate #1 Tellerette Tower Packing. Available at *www.verantis.com*; http://www.verantis.com/literature/12–10.10.pdf, accessed 2009.
38. Verantis Environmental Solutions Group. Pressure Drop vs. Gas Rate #2 Type-R Tellerette. Available at *www.verantis.com*; http://www.verantis.com/literature/12–10.11.pdf, accessed 2009.
39. Vereinigte Füllkörper-Fabriken GmbH & Co. KG. Your Expert for Tower Packing and Column Equipment, 2007.
40. QVF GmbH. Durapak Structured Borosilicate Glass Packings for Mass Transfer. Vol 12.05 P107e.1.
41. Schultes M. Raschig super-ring: a new fourth generation random packing. Paper presented at: 2001 Spring AIChE Meeting and Petrochemical and Refining Exposition, 2001; Houston, TX. April 21–26.
42. Koch-Glitsch LP. Intalox Packed Tower Systems: Metal Random Packing. Vol KGMRP-1 2M0303B. Wichita, 2003.
43. Koch-Glitsch LP. Intalox Packed Tower Systems: Structured Packing. Vol KGSP-1 2M0503E. Wichita, 2003.
44. Rhine-Ruhr, Inc. Dynapak Structured Column Packing. Vol Technical Information Sheet TI-03–05, Revision 2.
45. Rhine-Ruhr, Inc. Thermoplastic Dynaflow Rings. Vol Technical Information Sheet TI-03–10, Revision 1.
46. Koch-Glitsch, LP. Random Packing. Vol KRP-5 3M0600B. Wichita, 2000.
47. Koch Knight LLC. FLEXERAMIC Ceramic Structured packing Systems. Vol KCP-7 2M0303E, 2003.
48. Sherwood TK, Shipley GH, Holloway FAL. Flooding velocities in packed columns. *Ind Eng Chem*. 1938;30:765–769.
49. Lobo WE, Friend L, Hashmall F, Zenz F. Limiting capacity of dumped tower packings. *Trans Am Inst Chem Eng*. 1945;41:693–710.
50. Sarchet BR. Flooding velocities in packed towers. *Trans Am Inst Chem Eng*. 1942;38:283.
51. Leva M. Flow through irrigated dumped packings: pressure drop, loading, flooding. *Chem Eng Prog Symp Ser*. 1954;50:51–59.
52. Piché S, Larachi F, Grandjean BPA. Flooding capacity in packed towers: database, correlations, and analysis. *Ind Eng Chem Res*. 2001;40:476–487.
53. Woelee GF, Berends J. A capacity model for vertical pipes and packed columns based on entrainment. *Chem Eng J*. 2001;84:355–366.
54. Lockett MJ, Victor RA, Billingham JF. Structured packing flooding: its measurement and prediction. *IChemE Symp Ser*. 2006;152:400–408.
55. Hanley B. Dimensional analysis applied to the dependence of packing flood point on fluid physical properties. Paper presented at: AIChE Annual Meeting, 2001; Reno, NV. November 4–9.
56. Hanley B. Packed column hydraulics and continuous phase transitions. Paper presented at: AIChE Spring Meeting, 2010; San Antonio, TX. March 21–25.
57. Meier W, Stoecker WD, Weinstein B. Performance of a new, high efficiency packing. *Chem Eng Prog*. 1977:71.
58. Shaoting W, Zuoxiang Z, Xiyuan L. Investigation on rectifying characteristics of two new tower packings. *J Chem Ind Eng*. 1990;2:187–194.
59. Wu KY, Chen GK. Large-scale pilot columns and packed column scale-up. *IChemE Symp Ser*. 1987;104:B225–B245.
60. Kean JA, Turner HM, Price BC. Structured packing proven superior for TEG gas drying. *Oil Gas J*. 1991:41–46.
61. Billet R. Recent investigations of metal pall rings. *Chem Eng Prog*. 1967;63:53.
62. Fitz CW, Shariat A, Kunesh JG. Performance of structured packing in a commercial scale column at pressures of 0.02 to 27.6 bar. *Ind Eng Chem Res*. 1999;38:512–518.
63. Aspen Technology, Inc. Aspen Rate Based Distillation. 2010. Available at www.aspentech.com/products/aspen-ratesep.cfm, accessed June 24, 2010.
64. Hanley B, Shethna H. Improved mass transfer correlations for random and structured packings. Paper presented at: AIChE Spring Meeting and 6th Global Conference on Process Safety, 2010; San Antonio, TX. March 21–25.
65. Hanley B, Chen CC. Useful mass transfer correlations for packed towers. *AIChE J*. In press.
66. Renon H, Prausnitz JM. Local compositions in thermodynamic excess functions for liquid mixtures. *AIChE J*. 1968;14:135–144.
67. National Institute of Science and Technology. NIST Refprop description. 2009. Available at www.nist.gov/cstl/properties/fluids_modeling/refprop.cfm, accessed June 24, 2010.

Manuscript received Jan. 8, 2011, and revision received May 17, 2011.